HHS Public Access

Author manuscript

Arterioscler Thromb Vasc Biol. Author manuscript; available in PMC 2020 October 01.

Published in final edited form as:

Arterioscler Thromb Vasc Biol. 2019 October ; 39(10): 2157–2167. doi:10.1161/ATVBAHA.119.312922.

Calcification in human intracranial aneurysms is highly prevalent and displays both atherosclerotic and non-atherosclerotic types

Piyusha S. Gade, MS[1], **Riikka Tulamo, MD, PhD**[2], **Keewon Lee, PhD**[1], **Fernando Mut, PhD**[3], **Eliisa Ollikainen, MD, PhD**[5,9], **Chih-Yuan Chuang, MS**[9], **Bong Jae Chung, PhD**[4], **Mika Niemelä, MD, PhD**[5], **Behnam Rezai Jahromi, MD, PhD**[5], **Khaled Aziz, MD**[6], **Alexander Yu, MD**[6], **Fady T. Charbel, MD**[7], **Sepideh Amin-Hanjani, MD**[7], **Juhana Frösen, MD, PhD**[8], **Juan Cebral, PhD**[3], **Anne M. Robertson, PhD**[1,9]

[1]Department of Bioengineering, University of Pittsburgh, PA, USA [2]Department of Vascular surgery, Helsinki University Hospital and University of Helsinki, Helsinki, Finland [3]Department of Bioengineering, George Mason University, Fairfax, VA, USA [4]Department of Mathematical Sciences, Montclair State University, Montclair, NJ, USA [5]Department of Neurosurgery, Helsinki University Hospital and University of Helsinki, Helsinki, Finland [6]Department of Neurosurgery, Allegheny General Hospital, Pittsburgh, PA, USA [7]Department of Neurosurgery, University of Illinois at Chicago, Chicago, IL, USA [8]Department of Neurosurgery, Kuopio University Hospital, Kuopio, Finland [9]Department of Mechanical Engineering and Materials Science, University of Pittsburgh, PA, USA

Abstract

Objective—Although the clinical and biological importance of calcification is well recognized for the extracerebral vasculature, its role in cerebral vascular disease, particularly, intracranial aneurysms (IAs), remains poorly understood. Extracerebrally, two distinct mechanisms drive calcification, a non-atherosclerotic, rapid mineralization in the media and a slower, inflammation driven, atherosclerotic mechanism in the intima. This study aims to determine the prevalence, distribution and type (atherosclerotic, non-atherosclerotic) of calcification in IAs and assess differences in occurrence between ruptured and unruptured IAs.

Approach and Results—65 IA specimens (48 unruptured, 17 ruptured) were resected peri-operatively. Calcification and lipid pools were analyzed non-destructively in intact samples using high resolution (0.35μm) micro-CT. Calcification is highly prevalent (78%) appearing as micro (<500μm), meso (500μm - 1mm) and macro (>1mm) calcifications. Calcification manifests in IAs as both “non-atherosclerotic” (calcification distinct from lipid pools) and “atherosclerotic” (calcification in the presence of lipid pools) with three wall types: Type I - only calcification, no lipid pools (20/51, 39%), Type II - calcification and lipid pools, not co-localized (19/51, 37%),

Corresponding Author: Anne M. Robertson, **Address:** 440 Benedum Hall, 3700 O’Hara St, Pittsburgh, PA 15213, rbertson@pitt.edu, **O:** 412-624-9775, **F:** 412-624-4846.

Disclosure

FC: Transonic, Inc. Consultant (Significant); JC: Vascular Fluid Dynamics, Inc. (Modest).

Type III - calcification co-localized with lipid pools (12/51, 24%). Ruptured IAs either had no calcifications or had non-atherosclerotic micro- or meso-calcifications (Type I or II), without macro-calcifications.

Conclusion—Calcification in IAs is substantially more prevalent than previously reported and presents as both non-atherosclerotic and atherosclerotic types. Notably, ruptured aneurysms had only non-atherosclerotic calcification, had significantly lower calcification fraction and did not contain macro-calcifications. Improved understanding of the role of calcification in IA pathology should lead to new therapeutic targets.

Graphical Abstract

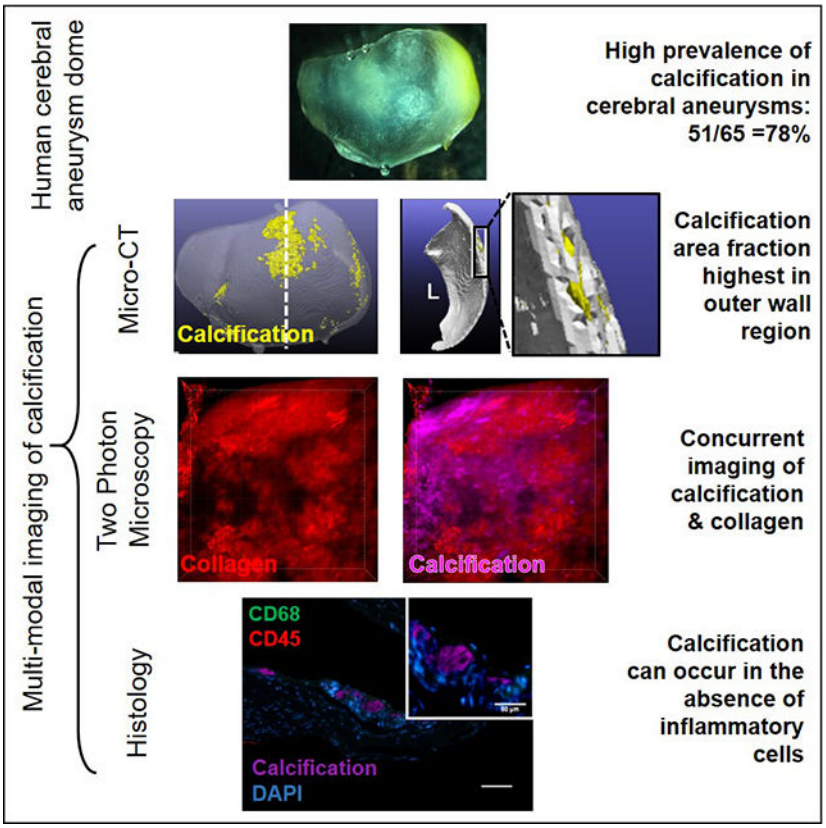

Keywords

Cerebral Aneurysms; Calcification; Micro-calcification; micro-CT

Introduction

Patient specific treatment planning for unruptured intracranial aneurysms (IAs) remains a complex issue for both clinical and scientific reasons. Clinically, there is a need to balance the risk of intervention with the potential risk of rupture[1–4]. The main morphological and anatomical factors that are clinically implicated in higher risk of IA rupture are posterior circulation[5], high aspect ratio[6], surface irregularities like lobulations[7], and size (>7mm)[4,7,8]. Although these factors correlate with increased risk, they are not exhaustive or specific

enough to impact clinical decision making for the vast majority of IAs. For example, while large IA size (>7mm) is often used as a metric of increased rupture risk, 38% of smaller IAs rupture[9] and there is no minimum size that alone guarantees structural integrity of the IA wall.

Aneurysms rupture when structural components of the wall, largely collagen fibers, are unable to withstand loading from transmural pressure. IA wall weakening is attributed to a variety of physical causes including enzymatic degradation of collagen fibers due to inflammation or wall remodeling, insufficient levels of collagen fiber deposition due to a dearth of intramural smooth muscle cells, and localized stress concentrations from, for example, calcifications in the IA wall[10–13]. This diversity of causes can confound current efforts to identify statistical associations between rupture risk and rupture related factors such as sac geometry and patient characteristics. Hence, there is a crucial need to complement current efforts with studies that directly look for physical causes of IA wall failure and identify the possibly distinct pathologies responsible for these wall changes.

It is well known that physical inclusions such as those formed from calcifications will alter the mechanical stress in a manner that is dependent on the inclusion size and material properties of the surrounding matrix[13–17]. The potential medical implications of these inclusions are seen, for example, in atherosclerotic lesions of extracranial arteries where micro-calcifications are associated with rupture of fibrous caps but macro-calcifications are associated with mechanical stability of the cap[17,18].

Vascular calcification is now known to arise from at least two different pathological processes which lead to different types of wall changes[19]. The most highly studied is a slow, inflammation driven, atherosclerotic type pathology of the intima with associated lipid pools[20] and the second is a non-atherosclerotic phosphate-dependent, rapid mineralization in the media[21–23]. Distinct therapies are needed for the prevention and possible reversal of these two types of calcification[24].

Despite these advances in understanding vascular calcification pathologies and recognition of their mechanical importance, the role of calcification in IA rupture has received limited attention, likely due to reports of a low prevalence between 1.7 – 29%[7,15,25]. However, these rates are based on clinical computed tomography (CT) imaging studies with a typical voxel resolution of 250–300μm that prevents the detection of micro-calcifications.

Our aim in this work is to determine the prevalence, distribution and type (atherosclerotic, non-atherosclerotic) of calcification in IAs and assess differences in occurrence between ruptured and unruptured IAs. We are able to leverage our database of peri-operatively resected human aneurysm samples and use high resolution *ex vivo* imaging techniques that directly image calcification as small as 3μm. As for extracerebral vessels, such knowledge can be leveraged for improved diagnosis and treatment methods once the role of calcification in IA pathology and mechanical strength are understood.

Materials and Methods

The data that support the findings of this study are available from the corresponding author upon reasonable request.

Aneurysm Tissue Harvesting

Aneurysm samples (n = 65) were harvested from aneurysm sacs in consented patients undergoing surgical clipping for treating unruptured (n = 48) and ruptured (n = 17) aneurysms. This study was approved by an Ethics Committee, protocol number IRB REN18010236. Samples were collected from three study sites – Alleghany General Hospital (Pittsburgh, PA, USA), University of Illinois at Chicago (Chicago, IL, USA), and Helsinki University Hospital (Helsinki, Finland). Samples from Alleghany General Hospital and University of Illinois at Chicago were transported in a dedicated cooled transport container to the University of Pittsburgh in a 0.9% (w/v) saline solution. Samples were then fixed using 4% paraformaldehyde or 3% glutaraldehyde. Samples from the Helsinki University Hospital were snap frozen in the operating room and transported to Pittsburgh after fixation in 10% formalin.

Patient Clinical Data

Patient clinical data was collected as previously described[12]. Briefly, patient age, gender, family IA history, smoking history, diagnosed hypertension, renal failure, diabetes and use of anti-thrombotic and statin medication were obtained from medical records. Patients were considered hypertensive if they were currently being treated for hypertension or if they were previously diagnosed with hypertension but declined treatment. Patients were categorized as non-smokers if they had never smoked cigarettes or had not smoked within the last 5 years. Patients who currently smoked or who had quit within the last 5 years were categorized as smokers. Patients were categorized as having renal failure if they were on dialysis or were either recommended/had previously undergone kidney transplant. Clinical patient data for indication of hypertension, smoking and anti-thrombotic medication was not available for 5,1, and 1 patient respectively. IA size, aspect ratio and presence of bleb/lobulations were calculated from 3D vascular models constructed from 3D rotational angiography or computed tomography angiography images as previously described[26]. Size was calculated from these reconstructed images as the total volume of the IA and aspect ratio as the ratio of aneurysm height and neck width[27]. Geometric parameters could not be analyzed for 11 patients due to the absence of imaging data for vascular reconstruction.

Micro-CT Scanning

Fixed aneurysm tissue samples (n = 65) were scanned using a high resolution (0.35μm) micro-CT scanner (Skyscan 1272, Bruker Micro-CT, Kontich, Belgium) at resolutions of at least 3μm (range: 1 – 3μm) depending on sample size to ensure that micro-calcifications of a minimum size (range of 3 – 9μm) could be captured. For scanning, samples were mounted on wet gauze to minimize dehydration and placed in a 1.5ml clear microcentrifuge tube. This tube was vertically mounted as previously described[28] to ensure the sample remained stationary. Samples were scanned at 50kV and 200μA with a frame averaging of 8, a rotation step size of 0.3 degrees, scanned 180 degrees around the vertical axis. Sample scanning time

was maintained at less than 2.5 hours to prevent sample dehydration. A 3D image of the sample was reconstructed using NRecon (Bruker Micro-CT, Kontich, Belgium) with an axial step size equal to the scanned pixel size.

Image Processing of Micro-CT data: Calcification and Lipid Pool Analysis

Aneurysm tissue and calcification mesh generation—The surface mesh used for analyzing the locations of calcification within the wall was created using Simpleware ScanIP (Synopsys, Mountain View, USA) as previously described[29,30]. Briefly, 3D reconstructed images from the micro-CT data were segmented into two distinct masks for the regions of calcification and non-calcified tissue. Tissue mask generation included segmentation, Gaussian smoothing, followed by morphological operations to remove surface noise, and connected components filtering. As previously described[30] and detailed in Supplementary Material, calcification was identified by elevated greyscale value relative to the tissue, validated using Alizarin Red staining in histological sections. The calcification mask was generated as previously described[30] using a combination of thresholding (Otsu multilevel thresholding filter) for segmentation and Boolean operations for subtraction of the calcification mask from the tissue mask. An unstructured triangular surface mesh was then generated for each component. Calcification and tissue volume fraction were calculated using the general properties module in ScanIP. The calcification mask was split into connected components to analyze individual calcification diameter, volume and eccentricity. Two particles connected by only a single vertex were considered to be separate particles, whereas a connection with one or more faces was considered to be a single particle.

Lipid pool analysis—As detailed in Supplementary Material, the presence or absence of lipids was determined from micro-CT images and confirmed by Oil Red-O staining of the corresponding histological sections. False positives by hemorrhage or capillaries were ruled out by consideration of greyscale, morphology and size. In particular, hemorrhage regions have a greyscale value similar to that of tissue which lies in the 50 – 80 greyscale regime[31]. Capillaries, if filled with blood, also appear at a similar intensity to that of tissue, thereby distinct from lipid pools and calcification. Additionally, capillaries are morphologically different (circular vs elliptical/irregular shaped) from lipid pools and have smaller diameters (5 – 10um) when compared with the smallest size of lipid pools identified (20um). Micro-CT images were then visually scored for the presence or absence of these lipid pools and their potential co-localization with calcification.

Wall Thickness Evaluation—Local wall thickness was assessed using a custom-written code as previously described[29]. Briefly, distance vectors were calculated from the inner to the outer surface elements and from the outer to the inner surface elements. Using these vectors, new “medial points” were introduced half way along these distance vectors. The wall thickness at the medial points was then approximated as the sum of the length of the distance vectors to each surface.

Calcification Location Analysis—Calcification was identified as located in the inner, middle or outer third of the wall using a previously developed approach[29]. Calcification location could not be analyzed for four samples for which the IA sample was collapsed,

preventing identification of the inner and outer surfaces across the entire sample in these cases.

Visual scoring of IA surface color

Calcification surface mesh was overlaid with the non-calcified tissue and compared with ex-vivo dissection scope images of resected IA samples[29]. The surface color of calcified regions was scored as either being colorless, white or yellow. If a sample presented calcification in multiple color regions, it was scored individually in each of the categories.

Histological and Multiphoton Analysis

To validate micro-CT findings of presence or absence of calcification and lipid pools, histological assessment was conducted on cerebral arteries and IA samples after micro-CT scanning and compared with micro-CT results. Tissue sections were stained with H&E, Alizarin red and Oil Red-O to examine cell presence, calcification and lipid respectively. Neutral lipid and free cholesterol content in IA samples was evaluated using BODIPY 493/503 (D3922, 2 μg/ml, Thermofisher Scientific, Waltham, MA) and filipin (F9765, 50 μg/ml, Sigma-Aldrich) stains, respectively. Inflammatory response was assessed by staining calcification positive sections with mouse anti-CD45 (clone 2B11 PD7/26, 3.75 μg/ml; Dako, Glostrup, Denmark), a leukocyte marker and mouse anti-CD68 (clone EBM11, 2.37 μg/ml; Dako)), a pan macrophage marker. Details of the protocol are provided in the Supplementary Material. Tonsil served as a positive control tissue for immunostainings. All histological images were captured with an inverted microscope (Eclipse Ti-E, Nikon Instruments, Melville, NY). To visualize the physical relationship between collagen fibers and calcification particles, intact aneurysm tissue samples were stained with OsteoSense 680EX (Perkin Elmer, Waltham, MA) and co-imaged with collagen using two photon microscopy with a recently developed protocol,[30] also outlined in the Supplementary Material.

Wall Classification for presence of calcification and lipid pools

IA walls were classified according to the association of calcification with lipid pools in micro-CT. Type I walls contained calcification without any lipid pools. In Type II walls, both calcification and lipid pools were detected, though never co-localized. In Type III walls, calcification could be found co-localized with lipid pools. Calcifications within and around lipid pools were referred to as “atherosclerotic” (Type III) as is normally seen in peripheral atherosclerosis[32], whereas calcifications distinct from lipid pools or found in the complete absence of lipid pools were referred to as a “non-atherosclerotic” (Types I and II). Calcification particles were subcategorized based on their size. Micro-calcifications were defined by diameters <500μm, meso-calcification by diameters between 500 – 1000 μm and macro-calcifications by diameters >1000 μm.

Statistical Analysis

Statistical analysis was performed using SPSS (IBM SPSS Statistics 25, IBM Corp, North Castle, NY). Proportions were calculated for categorical variables and χ^2 independence test or Fisher’s Exact test was used. For continuous variables, median and range or mean were

calculated and analyzed using Mann-Whitney U test or independent samples t-test. For normally distributed data, multiple group comparisons were performed using one or two-way ANOVA followed by the Tukey's post-hoc test. For data that violated the assumptions of parametric tests, multiple group comparison was performed using the Kruskal-Wallis test followed by the Mann-Whitney U test with a Bonferroni correction for post-hoc testing. The assumptions of normality and homogeneity of variance were tested using the Kolmogorov-Smirnov and Levene's test respectively.

Results

Human cerebral aneurysms exhibit high prevalence of calcification

High resolution micro-CT revealed the presence of calcification in 78% (51/65) of the IA samples. 60% of samples presented only calcification without associated lipid pools (Types I, II), Table I. We did not find any significant differences in patient characteristics between calcified and non-calcified samples. None of the patients in our cohort had renal failure and only 9% had type II diabetes. Furthermore, 57% of the IAs were harvested from the MCA and there was no statistical difference in location of the ruptured and unruptured samples.

Small, dispersed and large aggregated calcifications exist throughout the wall thickness

Calcification in the form of micro- and macro-calcifications were distributed in all three regions across the IA wall (Figure 1). Calcification in most samples occupied less than 0.1% of the sample volume (Figure 2A) and was approximately ellipsoidal in shape with an average aspect ratio of 0.39±0.21. 77.5% of calcified particles had a major diameter less than 30 μm. However, some calcified particles were as large as 3.87 mm (Figure 2B). For 70% of samples, no particular surface color was associated with calcification presence, even if calcification occupied a large volume fraction of the sample (Figure 1, row 1; Figure 2C, D). Calcification density, size (Supplementary Material, Figure III) and area fraction in IA wall all increased with an increasing distance from the lumen, with largest values in the outermost third of the wall (Figure 2E). Additionally, thicker regions in the IA wall tended to have calcification in the outer third of the wall, whereas thinner regions tended to possess calcification in the inner and middle thirds of the wall (Figure 2F). Thick and thin were defined relative to average thickness of the particular specimen.

Calcification found in atherosclerotic and non-atherosclerotic forms—Three IA wall types were identified (Figure 3); 39% (20/51) were Type I walls (calcification without any lipid pools; non-atherosclerotic calcification), 37% (19/51) were Type II walls (calcification that is never co-localized with lipid pools; non-atherosclerotic calcification) and 24% (12/51) were Type III walls (calcification co-localized with lipid pools; atherosclerotic calcification). When subcategorized by calcification particle size, samples with only micro-calcification were the most prevalent accounting for 65% (33/51) of calcified samples. Most micro-calcifications were substantially smaller than the 500 μm upper bound for this category. In particular, 97% of micro-calcifications were less than 90 μm and 78% were less than 30 μm in size. These micro-calcifications could be found either in clusters or as isolated particles (Figure 4C, D). All IA walls with meso- and macro-calcifications also included some (0.5 – 5%) dispersed micro-calcifications.

The existence of distinct non-lipid, non-inflammation associated calcification in the IA wall was confirmed in a region of Type II wall that had calcification without an associated lipid pool. The region was co-stained with lipid, free cholesterol and inflammatory markers. Both neutral lipids and free cholesterol were absent in the calcified region, as were inflammatory cells (Figure 4A, B) such as macrophages and leukocytes. Positive controls are shown in Supplementary Figure IV.

Factors associated with ruptured walls: Small calcification volume fraction, small calcification size and non-atherosclerotic calcifications

Ruptured IAs exhibited a lower calcification fraction than unruptured samples; a trend which existed across the three regions of the IA wall (Figure 5A). Furthermore, ruptured IAs did not contain macro-calcifications as opposed to unruptured IAs that possessed all sizes of calcification (Figure 5B).

Ruptured samples displayed only non-atherosclerotic calcification (calcification not associated with lipid pools- Types I, II) as opposed to unruptured samples which presented both atherosclerotic and non-atherosclerotic types (p=0.027). We did not find any significant differences in prevalence rates of either calcification or lipid pools between ruptured and unruptured samples, (Table I).

Discussion

This is the first analysis of the prevalence of micro through macro scale calcifications in the IA wall. We found very high prevalence rates of calcification in IA domes (78%), greater than previously reported in imaging[7,25] and histological[15] studies. We believe this difference is due to the high resolution (1–3μm) *ex vivo* imaging modality used here, which enabled direct, non-destructive evaluation of calcification across the entire intact sample, including particles in the 3–30μm size range.

This work is also the first to consider the possible existence of multiple mechanisms for calcification formation in the IA wall. Calcifications with and without associated lipid pools in extracranial arteries have already been shown to arise from distinct mechanisms. In particular, atherosclerotic intimal calcification of the extracranial arteries is found to be associated with later stages of an atherosclerotic process and is driven by lipid oxidation and inflammation. In contrast, the non-atherosclerotic medial calcification in extracranial arteries is not driven by a lipid oxidation induced inflammatory process but rather is attributed to aging as well as metabolite induced toxic changes that can arise from diseases such as renal insufficiency and diabetes mellitus[21,22].

Motivated by these results for atherosclerotic and non-atherosclerotic type calcification in extracranial arteries, we introduced three wall types (I-III) to describe calcified IA walls and categorized these as containing “atherosclerotic” or “non-atherosclerotic” calcification. Type I walls (only calcification, no lipid pools) and Type II walls (calcification and lipid pools, not co-localized) contained “non-atherosclerotic” calcification and accounted for 76% of all samples. Type III walls (include calcification that is located within or around lipid pools) are “atherosclerotic” and accounted for 23% of all samples. This Type III atherosclerotic pattern

is similar to later stage (type VII) atherosclerotic lesions in the classification of the American Heart Association (AHA) committee[32] where calcification is spatially associated with lipid pools and is formed through a lipid oxidation driven inflammatory process. Previous histological studies of the IA wall have shown that the SMC phenotype[33] as well as lipoprotein accumulation and associated foam cell formation[34,35] in the IA wall resemble changes accompanying peripheral atherosclerosis, further suggesting that some IA calcification shares common pathobiological mechanisms with calcification in atherosclerotic peripheral arteries.

While inflammation driven, atherosclerotic like calcification has previously been studied in IAs[34,35], the present work is the first to demonstrate calcification in IAs in the absence of lipids, suggesting a second mechanism of calcification formation is possible, potentially similar to non-atherosclerotic calcification in the medial layer of extracranial arteries. In contrast to extracerebral vessels, the non-atherosclerotic calcification was distributed across with entire IA wall. Cerebral arteries lack an external elastic lamina and the internal elastic lamina is additionally nearly universally missing in IAs. The absence of both these natural barriers in IAs could explain the more distributed nature of the non-atherosclerotic IA calcification compared with that in extracerebral vessels.

To further assess the possible similarity of this non-atherosclerotic presentation in IAs with non-inflammatory calcification in extracranial arteries, a region from a Type II wall with calcification distinct from lipid pools was analyzed for lipid and inflammatory markers (Figure 4A, B). The results confirmed that this calcification was not associated with lipids, cholesterol or inflammatory cells and was hence distinct from the typical atherosclerotic pathology outlined by the AHA. This non-inflammatory calcification in the IA wall was located near the IA lumen (Figure 4 A, B).

In order to understand the potential mechanism of non-atherosclerotic calcification formation, we assessed the prevalence of renal failure and type II diabetes in our patient cohort since these conditions have been implicated in extracerebral non-atherosclerotic calcification formation[21,22]. None of the patients in our cohort had kidney failure and only 9% had type II diabetes. Previous studies have also reported the existence of non-atherosclerotic calcification as a distinct form of calcification in the media of internal carotid arteries around the elastic lamina[36] and in peripheral artery disease[37]. Lanzer et al.[21] have conjectured that fragmented elastin can lead to such non-atherosclerotic calcification formation. Unpublished results from our group also show the presence of medial and adventitial calcification in control cerebral vessels. We therefore conjecture that at least some of the non-atherosclerotic calcification in the IA samples was formed due to the degradation of the elastic lamina in the cerebral artery prior to IA formation and would be exacerbated during IA formation. These findings suggest the need for future studies to understand the mechanism of non-atherosclerotic calcification formation. Building on the current work, an extensive evaluation of the prevalence, distribution and potential mechanisms of non-inflammatory calcification in IAs is the subject of ongoing investigation in our group.

Another important and marked finding in our study is that ruptured IAs had a lower calcification fraction and lacked macro-calcifications as compared to unruptured IAs. The role of calcification in rupture is a subject of ongoing investigations. In the extracerebral vasculature, computational modeling studies show that larger calcifications in plaques can contribute to load bearing and hence play a protective role[17,38–40]. Other studies have shown that plaque stress increases with increasing calcification, but only up to a certain limit, after which it plateaus or even reduces[41]. We surmise that larger plaques in IAs area can be protective against rupture, which would be consistent with the lack of larger plaques in ruptured IAs in our study. It has been conjectured that micro-calcifications could also play a mechanical role in rupture by generating regions of elevated stress (stress concentrations)[17] - leading, for example, to increased rupture risk in fibrous caps of extracranial arteries as well as in abdominal aortic aneurysms. Furthermore, the combined effect of collagen fibers, calcification and lipid pools on wall material properties ultimately dictates the mechanical behavior of soft tissues like the IA wall and this remains an ongoing area of investigation[13,16]

These potential differences in calcification pathologies and the expected mechanical role of calcification in wall vulnerability suggest a pressing need for further investigation of the multi-faceted role of calcification in the IA wall. We anticipate that calcification will impact IA wall strength through a direct mechanical role as noted above, as well as an indirect pathological role related to aneurysm wall remodeling. For example, the cluster of micro-calcifications seen in the Type II wall (Figure 4C, D) exists within a pocket of distinctly damaged collagen fibers. A structurally deficient region of this kind could potentially reduce the local wall strength, increasing vulnerability to rupture. Hutcheson et al. have also shown that micro-calcifications associate with regions of reduced collagen fibers, and conjecture that collagen acts a scaffold for calcification aggregation[42]. These findings also suggest that the pathology and mechanics of collagen-calcification interaction can determine IA wall strength. Further investigations of the role of calcification in pathological changes of this kind can leverage the recently developed protocols for simultaneous imaging of collagen fibers and calcification particles within intact samples[30]. These studies can be complemented by histological analysis of the IA wall to understand the indirect pathological role of calcification in IA wall remodeling.

The present study also sheds light on recent efforts to infer information about aneurysm walls from intraoperative images. In particular, due to difficulty in obtaining IA samples for analysis, intraoperative data on the aneurysm wall, such as color of the wall, are being collected as a possible surrogate markers of wall vulnerability[43,44]. In this context, it is important to note there was no association between the presence of micro, meso or macro-calcifications and color of the aneurysm wall, reflecting a challenge in using intraoperative visual data to assess calcification in the IA wall.

Limitations

Prior studies of combined occurrence rates for lipid droplets and pools in the IA wall based on histological sections, reported prevalence rates of almost 100%[34,35]. The high-resolution micro-CT used in the present work is able to identify lipid pools across intact IA specimens,

though is not suitable for resolving lipid droplets. Therefore, the prevalence rate of 57% for lipid pools is not directly comparable to the results of the prior studies and may reflect the lower threshold for detecting lipids and lipoproteins compared with different histological staining methods. Other limitations of our study include small sample size and selection bias. Tissue was harvested from the aneurysm sac after aneurysm neck clipping only when it was feasible for the patients. Additionally, all aneurysm samples represent only one moment in time in their pathogeneses. Therefore, chronological order of wall changes and causal relationships between the changes remain unclear in this study setting. Nevertheless, we made every effort to include all relevant patient and sample information in order to better understand the population under study.

Conclusion

In summary, we found calcification in intracranial aneurysms is substantially more prevalent than previously reported and manifests as both atherosclerotic and non-atherosclerotic types. Notably, ruptured IAs in this study had significantly lower calcification fraction in comparison with unruptured IAs, and only displayed non-atherosclerotic calcifications. Outside the brain, vascular calcification receives great focus as a potent player in mechanical stability of vessels and a target for pharmacological treatment[24]. Since no prior studies have assessed the prevalence, distribution or morphology of calcification in IAs with high resolution imaging modalities, there is an important gap in knowledge regarding even the presence of calcification in IA walls. Our study bridges this gap and provides a motivation for future lines of investigations into IA pathology and the role of calcification in IA wall rupture that can impact risk assessment and IA treatment.

Supplementary Material

Refer to Web version on PubMed Central for supplementary material.

Acknowledgments

Sources of Funding

This research was supported, in part, by a grant from the National Institutes of Neurological Disorders and Stroke (NINDS), NIH-1R01NS097457-01, the Finnish Medical Foundation, and an internal grant from Kuopio University Hospital (VTR 2017 and VTR2018).

Abbreviations

IA	Intracranial Aneurysm
CT	Computed Tomography

References

1. Juvela S, Korja M. Intracranial Aneurysm Parameters for Predicting a Future Subarachnoid Hemorrhage: A Long-Term Follow-up Study. Neurosurgery. 2017;81:432–440. [PubMed: 28327974]
2. Rinkel GJE, Djibuti M, Algra A, van Gijn J. Prevalence and Risk of Rupture of Intracranial Aneurysms: A Systematic Review. Stroke. 1998;29:251–256. [PubMed: 9445359]

3. Juvela S, Porras M, Poussa K. Natural history of unruptured intracranial aneurysms: probability of and risk factors for aneurysm rupture. J Neurosurg. 2008;108:1052–1060. [PubMed: 18447733]
4. International Study of Unruptured Intracranial Aneurysms Investigators. Unruptured intracranial aneurysms: natural history, clinical outcome, and risks of surgical and endovascular treatment. Lancet. 2003;362:103–110. [PubMed: 12867109]
5. Lall RR, Eddleman CS, Bendok BR, Batjer HH. Unruptured intracranial aneurysms and the assessment of rupture risk based on anatomical and morphological factors: sifting through the sands of data. Neurosurg Focus. 2009;26:E2.
6. Nader-Sepahi A, Casimiro M, Sen J, Kitchen ND. Is aspect ratio a reliable predictor of intracranial aneurysm rupture? Neurosurgery. 2004;54:1343–1348. [PubMed: 15157290]
7. The UCAS Japan Investigators. The Natural Course of Unruptured Cerebral Aneurysms in a Japanese Cohort. N Engl J Med. 2012;366:2474–2482. [PubMed: 22738097]
8. Korja M, Lehto H, Juvela S. Lifelong rupture risk of intracranial aneurysms depends on risk factors: A prospective Finnish cohort study. Stroke. 2014;45:1958–1963. [PubMed: 24851875]
9. Lindgren AE, Koivisto T, Björkman J, Fraunberg M, Helin K, Jääskeläinen JE, Frösen J. Irregular shape of intracranial aneurysm indicates rupture risk irrespective of size in a population-based cohort. Stroke. 2016;47:1219–1226. [PubMed: 27073241]
10. Hashimoto T, Meng H, Young WL. Intracranial aneurysms: links among inflammation, hemodynamics and vascular remodeling. 2011;193:118–125.
11. Aoki T, Kataoka H, Shimamura M, Nakagami H, Wakayama K, Moriwaki T, Ishibashi R, Nozaki K, Morishita R, Hashimoto N. NF- B Is a Key Mediator of Cerebral Aneurysm Formation. Circulation. 2007;116:2830–2840. [PubMed: 18025535]
12. Robertson AM, Duan X, Aziz KM, Hill MR, Watkins SC, Cebral JR. Diversity in the Strength and Structure of Unruptured Cerebral Aneurysms. Ann Biomed Eng. 2015;43:1502–1515. [PubMed: 25632891]
13. Robertson AM, Xinjie D, Maiti S, Thunes J, Cebral J, Aziz K, Frösen J, Gade PS, Tulamo R, Fortunato R, Charbel F, Amin-Hanjani S, Sang C. Role of calcification in aneurysm failure - a case study. Proc 5th Int Conf Comput Math Biomed Eng 10th-12th April Pittsburgh, PA, USA. 2017;1:52–55.
14. Buijs RVC, Willems TP, Tio RA, Boersma HH, Tielliu IFJ, Slart RHJA, Zeebregts CJ. Calcification as a risk factor for rupture of abdominal aortic aneurysm. Eur J Vasc Endovasc Surg. 2013;46:542–548. [PubMed: 24091093]
15. Nyström SHM. On factors related to growth and rupture of intracranial aneurysms. Acta Neuropathol. 1970;16:64–72. [PubMed: 5456388]
16. Volokh KY, Aboudi J. Aneurysm strength can decrease under calcification. J Mech Behav Biomed Mater. 2016;57:164–174. [PubMed: 26717251]
17. Vengrenyuk Y, Carlier S, Xanthos S, Cardoso L, Ganatos P, Virmani R, Einav S, Gilchrist L, Weinbaum S. A hypothesis for vulnerable plaque rupture due to stress-induced debonding around cellular microcalcifications in thin fibrous caps. Proc Natl Acad Sci. 2006;103:14678–14683. [PubMed: 17003118]
18. Otsuka F, Sakakura K, Yahagi K, Joner M, Virmani R. Has our understanding of calcification in human coronary atherosclerosis progressed? Arterioscler Thromb Vasc Biol. 2014;34:724–736. [PubMed: 24558104]
19. Demer LL, Tintut Y. Inflammatory, metabolic, and genetic mechanisms of vascular calcification. Arterioscler Thromb Vasc Biol. 2014;34:715–723. [PubMed: 24665125]
20. Stary HC. Natural history and histological classification of atherosclerotic lesions. Arterioscler Thromb Vasc Biol. 2000;20:1177–1178. [PubMed: 10807728]
21. Lanzer P, Boehm M, Sorribas V, Thiriet M, Janzen J, Zeller T, Hilaire CS, Shanahan C. Medial vascular calcification revisited: Review and perspectives. Eur Heart J. 2014;35:1515–1525. [PubMed: 24740885]
22. Amann K Media calcification and intima calcification are distinct entities in chronic kidney disease. Clin J Am Soc Nephrol. 2008;3:1599–1605. [PubMed: 18815240]

23. O'Neill WC, Han KH, Schneider TM, Hennigar RA. Prevalence of nonatheromatous lesions in peripheral arterial disease. Arterioscler Thromb Vasc Biol. 2015;35:439–447. [PubMed: 25477344]
24. Krohn JB, Hutcheson JD, Martínez-Martínez E, Aikawa E. Extracellular vesicles in cardiovascular calcification: Expanding current paradigms. J Physiol. 2016;594:2895–2903. [PubMed: 26824781]
25. Bhatia S, Sekula RF, Quigley MR, Williams R, Ku A. Role of calcification in the outcomes of treated, unruptured, intracerebral aneurysms. Acta Neurochir (Wien). 2011;153:905–911. [PubMed: 21286763]
26. Cebral JR, Castro MA, Appanaboyina S, Putman CM, Millan D, Frangi AF. Efficient pipeline for image-based patient-specific analysis of cerebral aneurysm hemodynamics: Technique and sensitivity. IEEE Trans Med Imaging. 2005;24:457–467. [PubMed: 15822804]
27. Sforza DM, Putman CM, Cebral JR. Hemodynamics of Cerebral Aneurysms. Annu Rev Fluid Mech. 2009;41:91–107. [PubMed: 19784385]
28. Cebral JR, Duan X, Gade PS, Chung BJ, Mut F, Aziz K, Robertson AM. Regional Mapping of Flow and Wall Characteristics of Intracranial Aneurysms. Ann Biomed Eng. 2016;44:1–15. [PubMed: 26620776]
29. Mut F, Gade P, Cheng F, Tobe Y. Combining data from multiple sources to study mechanisms of aneurysm disease: Tools and techniques. Int J Numer Meth Biomed Engng. 2018:1–18.
30. Gade P, Robertson A, Chuang C. Multiphoton Imaging of Collagen, Elastin and Calcification in Intact Soft Tissue Samples. Curr Protoc Cytom. 2017.
31. Wintermark M, Jawadi SS, Rapp JH, Tihan T, Tong E, Glidden DV, Abedin S, Schaeffer S, Acevedo-Bolton G, Boudignon B, Orwoll B, Pan X, Saloner D. High-resolution CT imaging of carotid artery atherosclerotic plaques. Am J Neuroradiol. 2008;29:875–882. [PubMed: 18272562]
32. Stary HC, Chandler a B, Dinsmore RE, Fuster V, Glagov S, Insull W, Rosenfeld ME, Schwartz CJ, Wagner WD, Wissler RW. A Definition of Advanced Types of Atherosclerotic Lesions and a Histological Classification of Atherosclerosis Atherosclerotic Lesion Types Advanced by Histology Type IV Lesions. Circulation. 1995;92:1355–1374. [PubMed: 7648691]
33. Coen M, Burkhardt K, Bijlenga P, Gabbiani G, Schaller K, Kövari E, Rüfenacht DA, Ruíz DSM, Pizzolato G, Bochaton-Piallat ML. Smooth muscle cells of human intracranial aneurysms assume phenotypic features similar to those of the atherosclerotic plaque. Cardiovasc Pathol. 2013;22:339–344. [PubMed: 23466011]
34. Ollikainen E, Tulamo R, Lehti S, Lee-Rueckert M, Hernesniemi J, Niemelä M, Yla-Herttuala S, Kovanen PT, Frösen J. Smooth muscle cell foam cell formation, apolipoproteins, and ABCA1 in intracranial aneurysms: Implications for lipid accumulation as a promoter of aneurysm wall rupture. J Neuropathol Exp Neurol. 2016;75:689–699. [PubMed: 27283327]
35. Frösen J, Tulamo R, Paetau A, Laaksamo E, Korja M, Laakso A, Niemela M, Hernesniemi J. Saccular intracranial aneurysm: Pathology and mechanisms. Acta Neuropathol. 2012;123:773–786. [PubMed: 22249619]
36. Vos A, Van Hecke W, Spliet W, Goldschmeding R, Isgum I, Kockelkoren R, Bleys R, Mali W, de Jong P, Vink A. Predominance of nonatherosclerotic internal elastic lamina calcification in the intracranial internal carotid artery. Stroke. 2016;47:221–223. [PubMed: 26514193]
37. Ho CY, Shanahan CM. Medial Arterial Calcification: An Overlooked Player in Peripheral Arterial Disease. Arter Thromb Vasc Biol. 2016;36:1475–1482.
38. Huang H, Virmani R, Younis H, Burke AP, Kamm RD, Lee RT. The impact of calcification on the biomechanical stability of atherosclerotic plaques. Circulation. 2001;103:1051–1056. [PubMed: 11222465]
39. Kiousis DE, Rubinigg SF, Auer M, Holzapfel GA. A Methodology to Analyze Changes in Lipid Core and Calcification Onto Fibrous Cap Vulnerability: The Human Atherosclerotic Carotid Bifurcation as an Illustratory. J Biomech Eng. 2019;131:1–9.
40. Wong KK, Thavornpattanapong P, Cheung SC, Sun Z, Tu J. Effect of calcification on the mechanical stability of plaque based on a three-dimensional carotid bifurcation model. BMC Cardiovasc Disord. 2012;12:7. [PubMed: 22336469]
41. Teng Z, Brown AJ, Calvert PA, Parker RA, Obaid DR, Huang Y, Hoole SP, West NEJ, Gillard JH, Bennett MR. Coronary Plaque Structural Stress Is Associated With Plaque Composition and

Subtype and Higher in Acute Coronary Syndrome The BEACON I (Biomechanical Evaluation of Atheromatous Coronary Arteries) Study. Circ Cardiovasc Imaging. 2014;7:461–470. [PubMed: 24557858]

42. Hutcheson JD, Goettsch C, Bertazzo S et al. Genesis and growth of extracellular vesicle derived microcalcification in atherosclerotic plaques. Nat Mater. 2016;15:335–343. [PubMed: 26752654]
43. Sugiyama SI, Niizuma K, Nakayama T, Shimizu H, Endo H, Inoue T, Fujimura M, Ohta M, Takahashi A, Tominaga T. Relative residence time prolongation in intracranial aneurysms: A possible association with atherosclerosis. Neurosurgery. 2013;73:767–776. [PubMed: 23863763]
44. Tobe Y Pathological Engineering for Predicting Transition of Human Cerebral Aneurysms. 2016.

Highlights

- This is the first study using high resolution micro-CT to analyze calcification in human IAs and found a substantially higher prevalence of calcification (78%) than previously reported using clinical scanners.
- Three categories of IA calcification were found with respect to localization with lipids: Type I – only calcification, no lipid pools (20/51, 39%), Type II – calcification and lipid pools, not co-localized (19/51, 37%), Type III – calcification co-localized with lipid pools (12/51, 24%).
- While inflammation driven, atherosclerotic type calcification has previously been studied in IAs, the present work is the first to demonstrate a second mechanism of calcification in IAs with features similar to non-inflammatory calcification in extracranial arteries.
- Ruptured and unruptured IAs showed substantially different presentation. In contrast to unruptured IAs, ruptured aneurysms had significantly lower calcification fraction and contained only non-atherosclerotic micro and meso-calcifications.

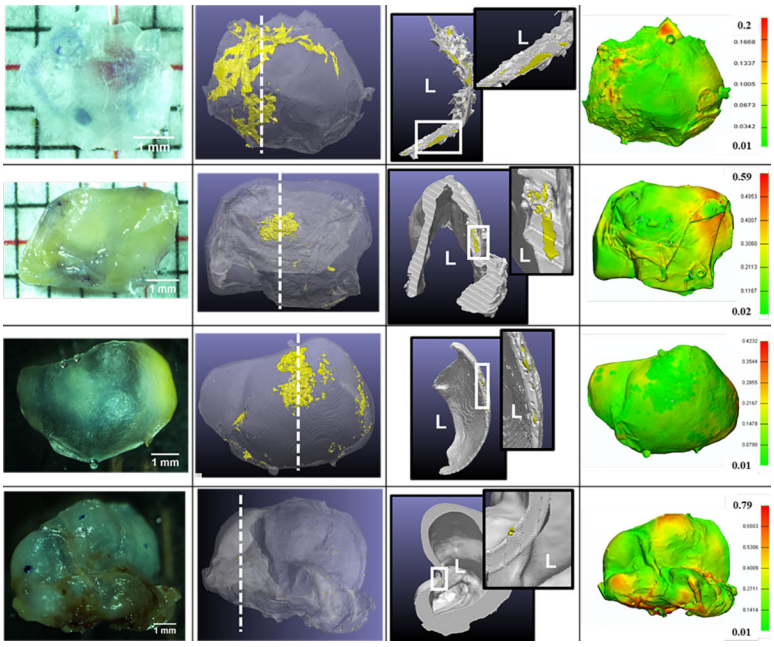

Figure 1:

Diversity of calcification morphology, location and tissue surface appearance as seen with high resolution micro-CT for four representative aneurysm samples (Rows 1–4). 3D reconstructed and cross-section images of the micro-CT scans show calcification in yellow and non-calcified tissue in grey. Cross section images are taken at locations indicated by a dashed white line in the 3D reconstruction image. L indicates lumen and insets show calcified region at higher magnification. Wall thickness contours are in mm.

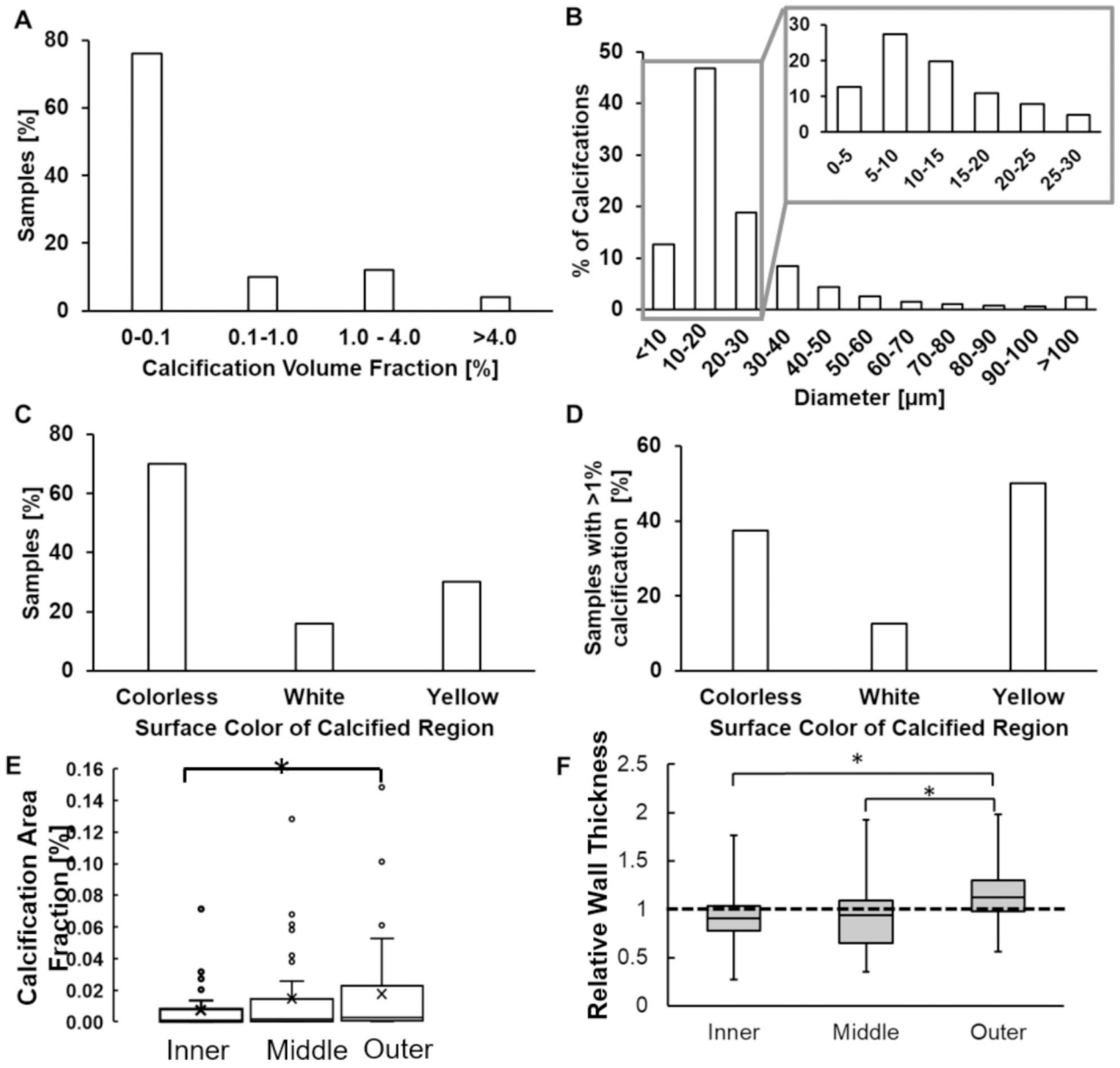

Figure 2:

Calcification in human IAs (A) occupies less than 0.1% of sample wall volume, (B) exists mostly as small (< 30μm) micro-calcifications which can exist in clusters and (C, D) does not associate with any specific tissue surface color even when it occupies a large volume.(E) Calcification area fraction increases with increasing distance from lumen ($p = 0.016$; $n = 50$). (F) Calcification in the outer third of the wall is found in regions of high relative wall thickness - the ratio of thickness in the calcified region relative to average wall thickness for that specimen ($p = 0.0001, 0.0001$; $n = 50$) whereas calcification in the inner and middle layer occurs in region of average wall thickness. A relative wall thickness of 1 indicates the calcified wall region has a thickness equal to the average wall thickness of the particular specimen.

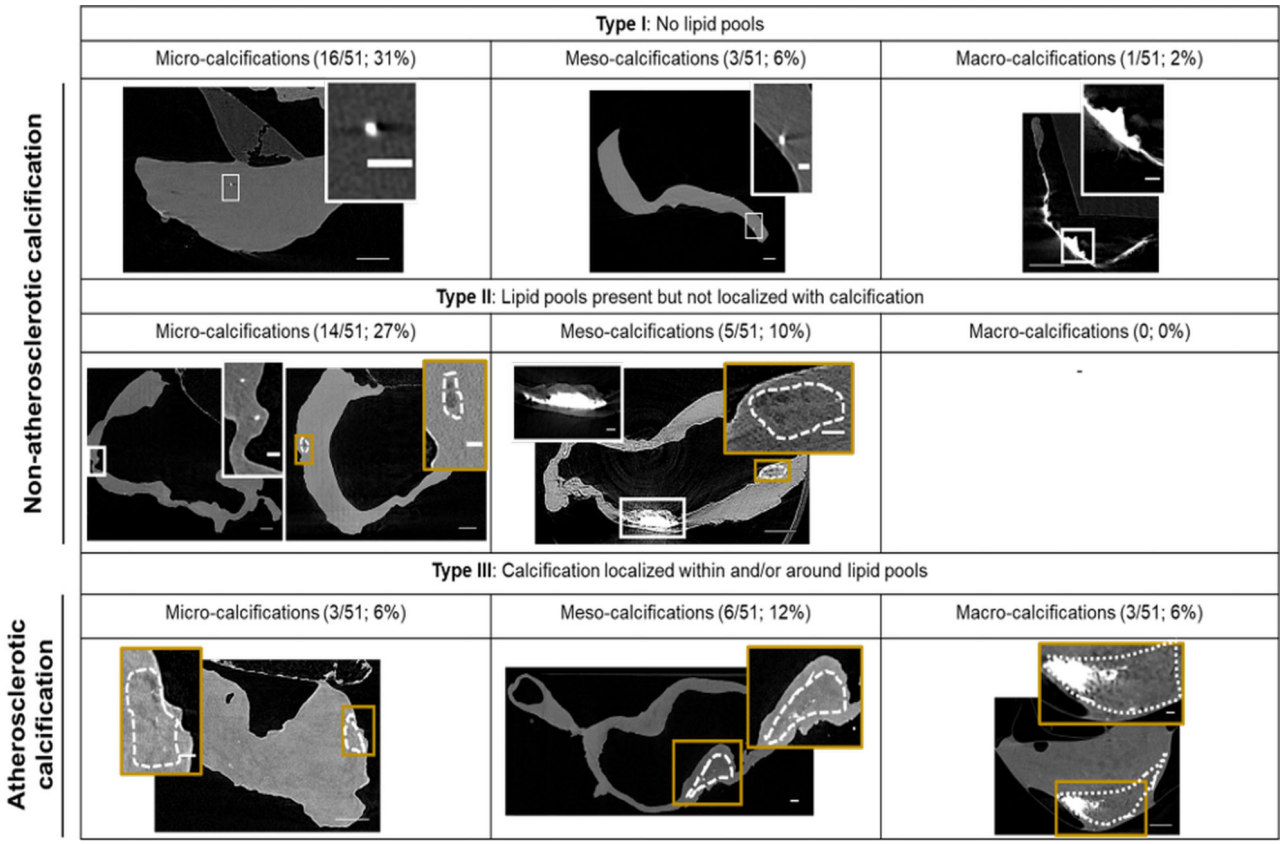

Figure 3:

Three main wall types found in aneurysm samples based on the relationship between calcification and lipid pools. Cross-section micro-CT images of representative calcified wall types present in IAs. Dotted regions indicate lipid pools. White and gold inset images show calcification and lipid pools, respectively, at high magnification. Scale bars correspond to 500μm for main images and 100μm for inset images. L indicates lumen.

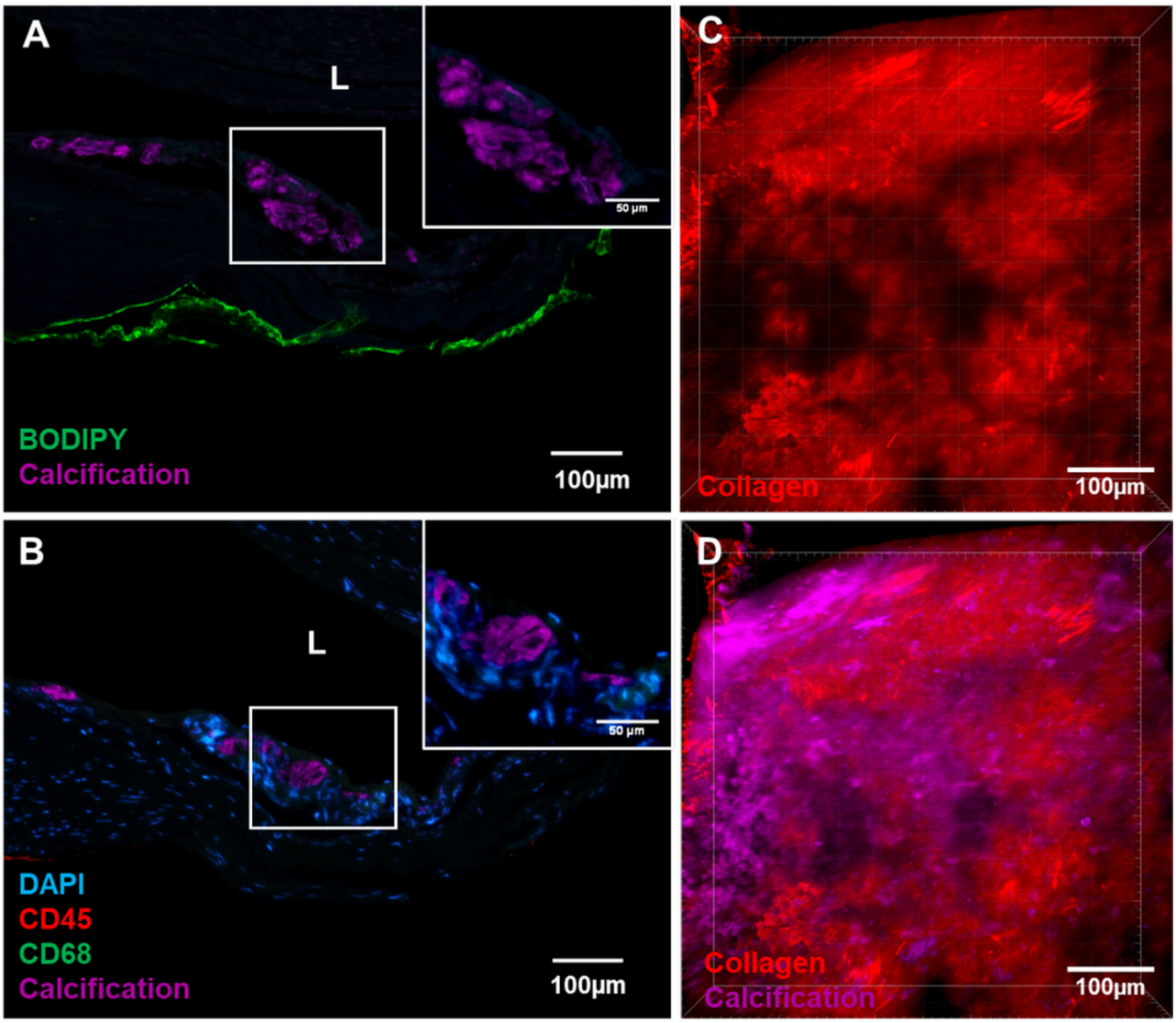

Figure 4:

A region from a Type II wall presenting a non-atherosclerotic calcification region without an associated lipid pool. (A) Calcification (stained with OsteoSense) did not localize with neutral lipid (stained with BODIPY) or free cholesterol (stained with filipin) as typically seen in atherosclerotic plaques. (B) Inflammatory response was also absent as indicated by the absence of both CD45 stained pan leukocyte marker and CD68 stained macrophages at the calcified area. Co-imaging of the relationship between collagen fibers and calcification particles under MPM showed (C) damaged regions of wall devoid of collagen fibers (red signal from second harmonic generation) were (D) filled with clusters of calcification particles (magenta, stained with Ostoesense).

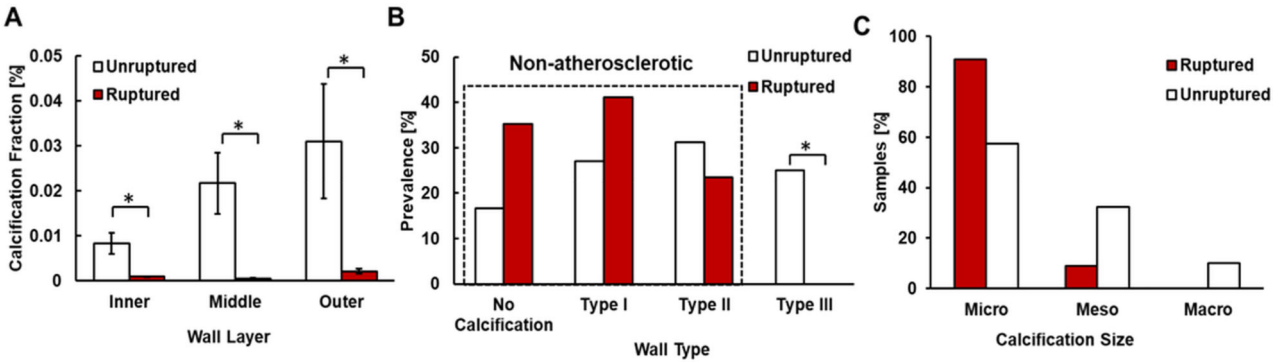

Figure 5:

(A) Ruptured walls have significantly lower calcification fraction than unruptured walls in human IAs, p = 0.005, 0.006, 0.029 for inner, middle and outer thirds of the wall, respectively (n = 50). (B) Ruptured IAs are limited to either having no calcifications or “non-atherosclerotic” calcifications (Type I and Type II walls). No ruptured IAs display “atherosclerotic” calcifications (Type III walls) (p = 0.027*). (C) with micro or meso-calcifications, or Type II walls only with micro-calcifications (n=65), whereas unruptured walls possess all wall types.

Table I:

Patient characteristics and prevalence rates for calcification and lipid pools.

	Total (n=65)	Unruptured (n=48)	Ruptured (n=17)	p value
Patient Clinical Characteristics				
Age (years)	57.50 (30 – 79)	58 (30 – 79)	54 (43 – 66)	0.089
Female Sex (%)	50/65 (77)	36/48 (75)	14/17 (82)	0.741
Family History for IAs (%)	15/65 (23)	13/48 (27)	2/17 (12)	0.478
Smoker (%)	23/65 (35)	17/48 (35)	6/17 (35)	1.000
Hypertensive (%)	28/65 (44)	21/48 (44)	7/17 (41)	1.000
Anti-thrombotic medication (%)	14/65 (22)	14/48 (29)	0/17 (0)	0.024 *
Statins (%)	16/65 (25)	15/48 (31)	1/17 (6)	0.086
Type II Diabetes	6/65 (9)	5/48 (10)	1/17 (6)	1.000
Size [mm^3]	7.6 (4.6 – 15.6)	7.6 (4.6 – 14.5)	9.2 (4.8 – 15.6)	0.642
Aspect Ratio	1.06 (0.4 – 3.6)	1.05 (0.5 – 2.0)	1.18 (0.4 – 3.6)	0.509
Blebs/Lobulations	19/65 (29)	13/48 (27)	6/17 (35)	0.298
Location				
MCA	37/65 (57)	29/48 (60)	8/17 (47)	0.563
ICA	8/65 (12)	7/48 (15)	1/17 (6)	0.667
ACOM	8/65 (12)	6/48 (13)	2/17 (12)	1.000
PCOM	6/65 (9)	3/48 (6)	3/17 (18)	0.159
Others ¥	5/65 (8)	3/48 (6)	2/17 (12)	0.592
Prevalence Rates of Calcification and Lipid Pools in IAs				
Calcification (%)	51/65 (78)	40/48 (83)	11/17 (65)	0.167
Lipid pools (%)	39/65 (60)	29/48 (60)	10/17 (59)	0.783
Both calcification and lipid pools (%)	30/65 (46)	25/48 (52)	5/17 (29)	0.158
Wall Type I, II (“Non- atherosclerotic calcification”)	39/65 (60)	28/48 (58)	11/17 (65)	0.380
Wall Type III (“Atherosclerotic calcification”)	12/65 (18)	12/48 (25)	0/17 (0)	0.027 *

Median and range are given for continuous variables.

* P<0.5 (X^2, Fisher’s Exact Test or Mann-Whitney U test).

¥ Other aneurysm locations in this study with a single case include ruptured aneurysms: BA tip, PICA; and unruptured aneurysms: ACA, PCOM-ICA, VA.

Abbreviations used: MCA = Middle Cerebral Artery, ICA = Internal Carotid Artery, ACOM = Anterior Communicating Artery, PCOM = Posterior Communicating Artery, BA = Basilar Artery, PICA = Posterior Inferior Cerebellar Artery, ACA = Anterior Cerebral Artery, VA = Vertebral Artery.